Electronic supplementary information (ESI)

Aggregation-based growth of faceted $Bi_2Fe_4O_9$ micro-cuboid with a remarkable visible light photo-Fenton catalytic activity

Wensen Gao, Lingfeng Tang, Min Zhu, Yongfeng Yuan, Shaoyi Guo and Simin Yin*

School of Mechanical Engineering, Zhejiang Sci-Tech University, 310018, Hangzhou, P.R. China.

*E-mail: yinsm@zstu.edu.cn.

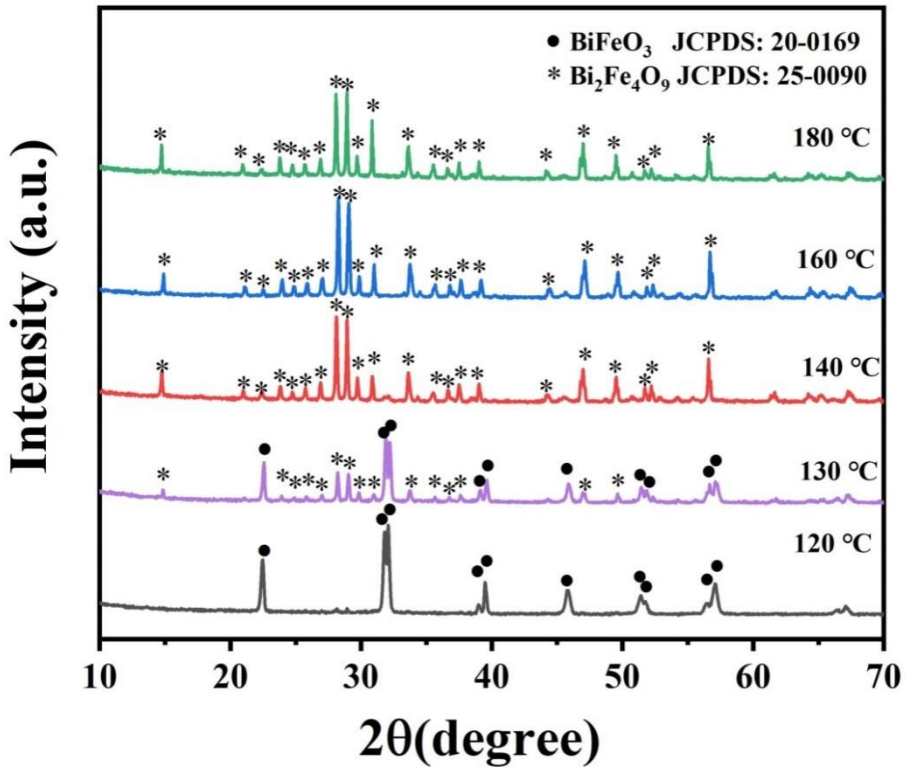

Fig. S1 XRD patterns of the samples hydrothermally synthesized for 12h at different temperature: (a)120℃, (b)130℃, (c) 140℃, (d)160℃ and (e)180℃ with Bi: Fe=1:2.

Fig. S1 shows XRD patterns of the as-synthesized products at 120, 130, 140, 160 and 180 °C for 12h with Bi: Fe molar ratio of 1:2 and NaOH concentration of 10M. Pure phase $BiFeO_3$ (JCPDS: 20-0169) was obtained at 120 °C, and $Bi_2Fe_4O_9$ (JCPDS: 25-0090) started to appear when reaction temperature was increased to 130 °C. With a further increase of the hydrothermal reaction temperature to above 140 °C, the resultant sample products only consist of pure phase

$Bi_2Fe_4O_9$ (JCPDS: 25-0090) with strong diffraction peaks, indicating good crystallinity of the products. It is revealed that $BiFeO_3$ (JCPDS: 20-0169) phase can be obtained at a moderate reaction temperature, whereas, the formation of $Bi_2Fe_4O_9$ (JCPDS: 25-0090) phase could be observed at the temperature above 140 ^oC.

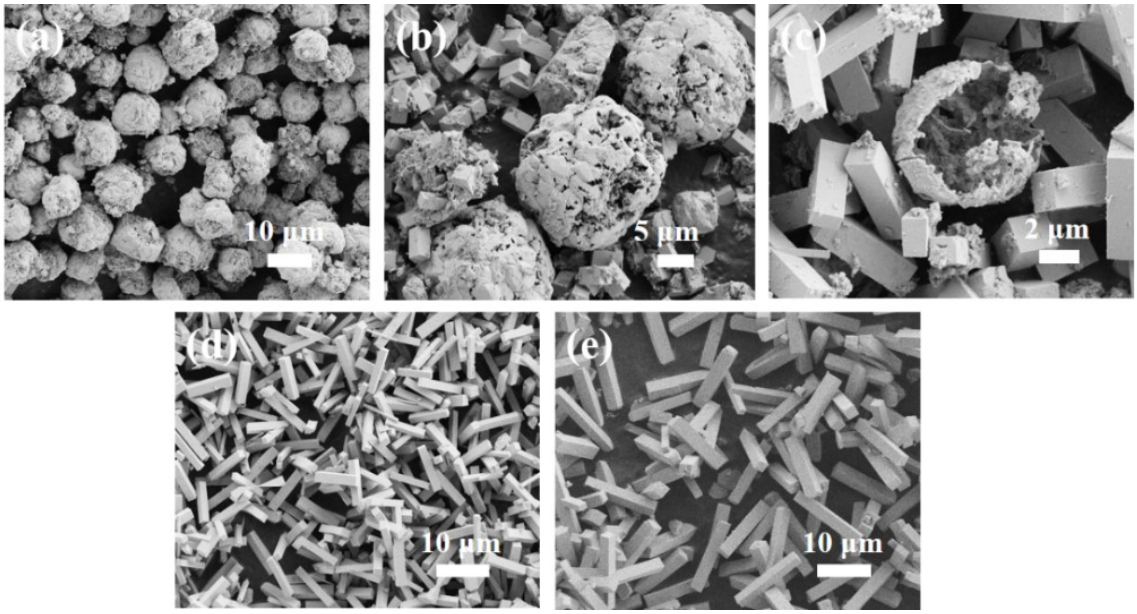

Fig. S2 SEM images of the samples hydrothermally synthesized for 12h at different temperature: (a)120℃, (b)130℃, (c) 140℃, (d)160℃ and (e)180℃ with Bi:Fe=1:2.

Fig. S2 exhibits the corresponding SEM images of bismuth ferrites synthesized with increasing hydrothermal temperatures. At a mild reaction temperature of 120 ^oC, monodispersed micro-spheres with a radius size of~ 10 μm could be observed, which should be the $BiFeO_3$ (JCPDS: 20-0169) phase according to Fig. S1. With the reaction temperature increased to 130 ^oC, the density of micro-spheres started to decrease to form hollowed micro-spheres and micro-rods (length of ~5 μm) started to appear, as presented in Fig. S2(b). When reaction temperature increased to 140 ^oC, the $BiFeO_3$ (JCPDS: 20-0169) microspheres were further dissoluted and becomes hollow spheres with a more loosen structure, and free-standing $Bi_2Fe_4O_9$ (JCPDS: 25-0090) micro-cuboids formed in a large quantity, as in Fig. 2S(c). Further increasing the temperature to 160 and 180 ^oC, mono-dispersed and free-standing $Bi_2Fe_4O_9$ (JCPDS: 25-0090) micro-cuboids (length of ~10 μm) with well-defined smooth surface could be observed in the corresponding resultant products, as in Fig. 2S (d) and (e), and no other morphology could be

observed. From the above analysis, it is demonstrated that the morphology variation from perovskite $BiFeO_3$ (JCPDS: 20-0169) micro-spheres to mullite $Bi_2Fe_4O_9$ (JCPDS: 25-0090) micro-cuboids is a dynamically consecutive process and the growth of $Bi_2Fe_4O_9$ (JCPDS: 25-0090) micro-cuboids is on the basis of the uninterrupted dissolution of $BiFeO_3$ (JCPDS: 20-0169) micro-spheres.

Table S1 The summary of hydrothermal synthetic conditions and phase structure of the as-synthesized powder samples at different hydrothermal time.

NaOH concentration(M)	Molar ratio of Bi:Fe	Reaction temperature(°C)	Reaction time(h)	Phase structure
10	1:2	180	0.5	Pure phase $Bi_{25}FeO_{40}$,
10	1:2	180	1	Pure phase $BiFeO_3$
10	1:2	180	1.5	$BiFeO_3$+$Bi_2Fe_4O_9$
10	1:2	180	2	$BiFeO_3$+$Bi_2Fe_4O_9$
10	1:2	180	6	$BiFeO_3$+$Bi_2Fe_4O_9$
10	1:2	180	12	Pure phase $Bi_2Fe_4O_9$

In order to clearly compare the effects of reaction time on the morphology and phase evolution of bismuth ferrites, the detailed hydrothermal conditions and phase structures were investigated and summarized in Table S1. The results show the chemical composition of the as-synthesized hydrothermal products was changing with reaction time. When hydrothermal time is as short as 0.5h, only pure phase $Bi_{25}FeO_{40}$ (JCPDS: 46-0416) micro-particles with lateral size of ~ 10 um were observed. When the reaction time was increased to 1h, pure phase $BiFeO_3$ (JCPDS: 20-0169) microspheres with radius of ~3 um were formed, indicating that the 0.5h-sample of pure phase $Bi_{25}FeO_{40}$ are highly active precursor species and can be turned thoroughly into $BiFeO_3$ in a relatively short time. With the increase of reaction time to 1.5 h~6 h, crystalline $Bi_2Fe_4O_9$ (JPCDS: 25-0090) started to appear in the corresponding resultant product. And the crystallinity becomes stronger with reaction time being increased at the expense of $BiFeO_3$ microspheres. Finally when

reaction time reaches 12 h, $BiFeO_3$ microspheres were dissolved totally and turned into pure phase $Bi_2Fe_4O_9$ (JPCDS: 25-0090) micro-cuboids. Thus, until now mullite $Bi_2Fe_4O_9$ (JPCDS: 25-0090) micro-crystals were successfully synthesized by controlling the hydrothermal reaction time.

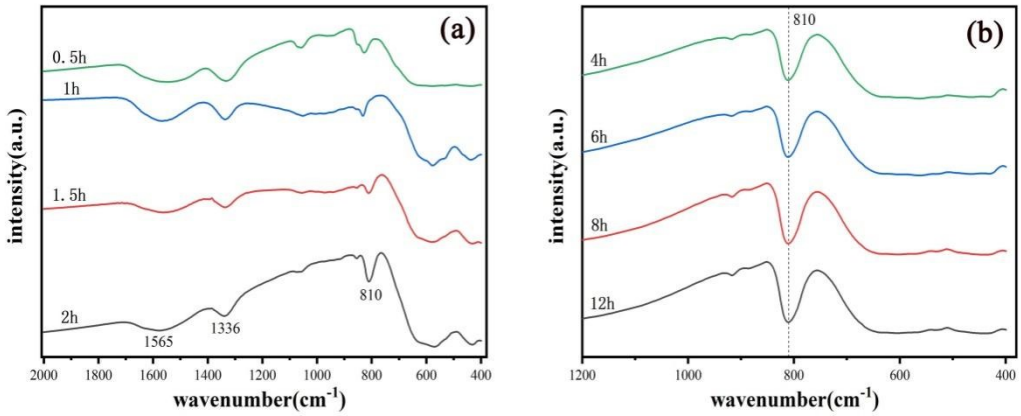

Fig. S3 FT-IR transmittance spectra in the 2000-400 cm^{-1} of samples hydrothermally synthesized with Bi:Fe molar ratio =1:2 at 180 ^oC for different reaction time: 0.5h ~ 12h.

Herein, FT-IR spectroscopy was employed to characterize the surface chemical bonds of time-related hydrothermal products. As presented in Fig. S3, when hydrothermal reaction time ranges from 0.5 h to 2 h, the FT-IR transmittance spectra of the products show mainly three band groups in the ~1565 cm^{-1} (assigned to -OH stretching vibration and H-O-H bending stretching of the adsorbed H_2O molecules), ~1336 cm^{-1} (ascribed to carboxyl C-OH stretching) and ~810 cm^{-1} (Fe-O stretching vibration of the FeO_4 tetrahedral unit), respectively. Noted that with the elongation of the hydrothermal reaction time from 4 h to 12 h, the transmittance spectra of the samples at ~810 cm^{-1} become sharper and more remarkable, indicating a stronger stretching vibration of the FeO_4 unit.[1,2] Further, from 6 h to 12 h products, the transmittance spectra exhibited similar strong peaks at ~810 cm^{-1}, indicating a pure-phased $Bi_2Fe_4O_9$ sample system without impurities was obtained.

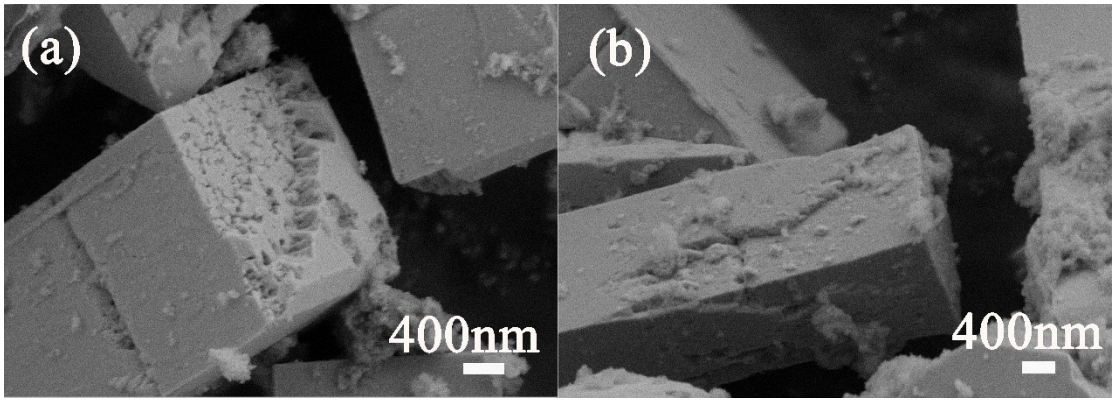

Fig. S4 SEM images of samples hydrothermally synthesized for 1.5h (Hydrothermal conditions: 180°C, Bi: Fe = 1:2, 10M NaOH; denoted as: S1.5h)

Fig. S4 shows the SEM images of S1.5h sample, bismuth ferrites micro-rods with clear cross-section surfaces and fluffy side surfaces exposed. It can be observed that the as-synthesized micro-rods exhibited a rough surface of the cross-section consisted of small particles, indicating a nanoparticles-assembly in a specific manner and a subsequent crystallization process.

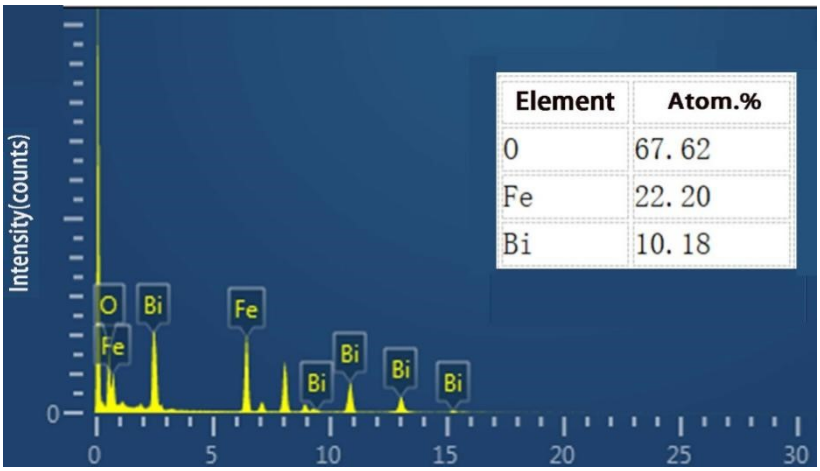

Fig. S5 Elemental distribution of the as-synthesized $Bi_2Fe_4O_9$ micro-cuboid sample.

Fig. S5 shows the total energy spectrum of the S10M micro-cuboid ($Bi_2Fe_4O_9$). The insert is the atomic percentage of Bi, Fe and O elements of the resultant products. The elemental composition of the S10M sample corresponds well to the chemical formula of the components.

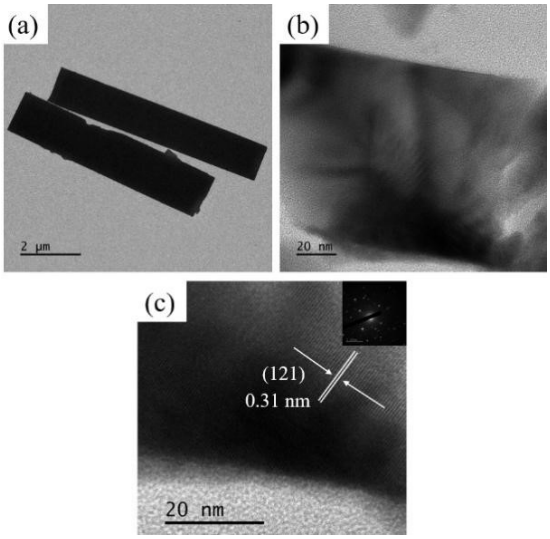

Fig. S6 Low magnification TEM image of (a) monodispersed $Bi_2Fe_4O_9$ micro-cuboids, (b) cross-section of epoxy-resin embedded $Bi_2Fe_4O_9$ sample and (c) corresponding HRTEM image of the sample.

Fig. S6 shows the TEM and HRTEM images of the monodispersed $Bi_2Fe_4O_9$ micro-cuboid sample. In Fig. S6(a), it can be observed that the as-prepared $Bi_2Fe_4O_9$ sample presents a cuboid-like shape with lateral size of~ 8-10 μm in the long direction and lateral size of 1-2 μm at the end. The surface of the $Bi_2Fe_4O_9$ micro-cuboid is smooth with a standard square-like configuration in the end. Fig. S6 (b) presents the morphology of the cross-section of $Bi_2Fe_4O_9$ sample by epoxy-resin embedding treatment. And the lattice spacing of 0.31 nm in Fig. S6 (c) corresponding to the (121) facet of mullite $Bi_2Fe_4O_9$ micro-cuboid (JCPDS: 25-0090) is observed clearly.

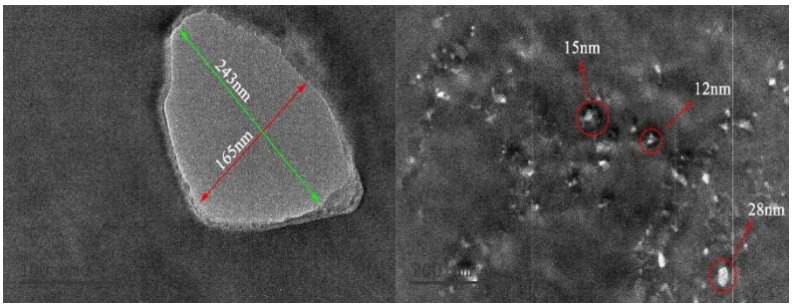

Fig. S7 Low magnification TEM images of the cross-section of $Bi_2Fe_4O_9$ micro-cuboid sample from FIB treatment.

The TEM images show the microstructure of the cross-section of the as-prepared $Bi_2Fe_4O_9$ micro-cuboid slice sample by FIB treatment. It is clear that a large pore with a diameter of 160-

200 nm, and a group of smaller pores with diameter of~15-30 nm can be observed in the cross section of the $Bi_2Fe_4O_9$ sample, displaying a porous structure of the sample. The result provides evidence that the as-prepared $Bi_2Fe_4O_9$ micro-cuboid experienced a crystallization process from surface to inside section, which is consistent with that of Fig. 5. This results combined with that of Fig. 3, 4 and 5 could further demonstrate that the as-synthesized $Bi_2Fe_4O_9$ micro-cuboid exhibits a porous structure inner side with a smooth and well-defined surface outside.

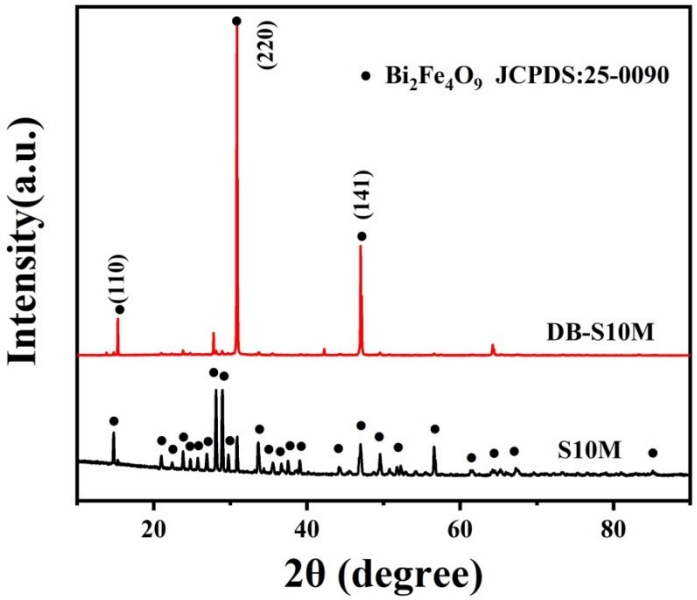

Fig. S8 XRD patterns of the $Bi_2Fe_4O_9$ micro-cuboids hydrothermally synthesized at 180 °C for 12 h (S10M, in black) and its corresponding doctor-blade sample (DB-S10M, in red).

Fig. S8 presents the XRD patterns of the as-synthesized S10M sample and its doctor-blade sample. It can be observed that all the diffraction peaks can be assigned to that of $Bi_2Fe_4O_9$ standard powder diffraction (JCPDS: 25-0090) as shown in S10M sample in black, with (001), (121) and (211) to be the three strong diffraction peaks. In comparison, the XRD pattern of the sample of DB-S10M, the relative intensities of the (110), (220) and (141) peaks to those of other peaks are greatly enhanced, suggesting that more (110), (220) and (141) facets meet Bragg's law and exposed as a result of the alignment of $Bi_2Fe_4O_9$ micro-cuboids after compression of the power sample prepared in the XRD test. From the above, it could be reasonably deduced that the $Bi_2Fe_4O_9$ micro-cuboids are well-crystallized and faceted single crystals with (110) and (-110) as the major side facets exposed.

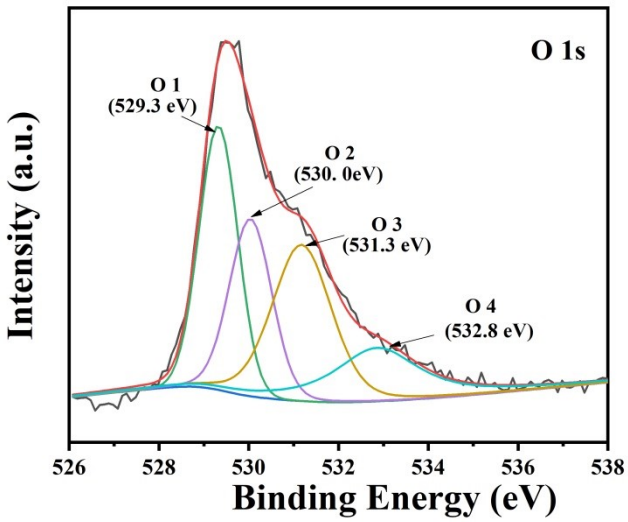

Fig. S9 XRD patteHigh resolution XPS spectrum of O 1s of $Bi_2Fe_4O_9$ micro-cuboid sample.

Fig. S9 presents the O1s profile of $Bi_2Fe_4O_9$ micro-cuboid sample. It can be deconvoluted into four peaks at ~529.3 eV, 530.0 eV, 531.3 eV and 532.8 eV, which can be ascribed to lattice Bi-O-Fe bonds, surface lattice oxygen, the existence of oxygen vacancies and absorbed H_2O or surface carbonate.[3]

Table S2 The magnetic properties of $Bi_2Fe_4O_9$ samples hydrothermally synthesized under different NaOH conditions at 300K.

Samples	M_s (emu/g)	Hc (O_e)
S10M	0.86	402
S12M	0.76	235
S14M	0.49	225

All the samples were measured at 300K in the magnetic field range from -20000 O_e to 20000 O_e. The magnetization values of the samples S10M, S12M and S14M are 0.86 emu/g, 0.76 emu/g and 0.49 emu/g 0.43239 emu/g, respectively, as listed in Table S2.

References

[1] Z. T. Hu, B. Chen and T. T. Lim , *RSC Adv.*, 2014, **4**, 27820.

[2] Z. T. Hu, Z. Chen, R. Goei, W. Y. Wu and T. T. Lim, *Nanoscale*, 2016, **8**, 12736-12746.

[3] M. Razavi, A. Barras, M. Ifires, A, Swaidan, M. Khoshkam, S. Szuneritts, M. K. Zareh and R. Boukherroub, *J. Colloid. interf. Sci.*, 2022, **613**, 384-395.